Plasmonics (2023) 18:1467–1476
https://doi.org/10.1007/s11468-023-01862-5

RESEARCH

Plasmonic Modulator Based on Graphene and Dual Back-to-Back U-Shaped Silicon Waveguide for Optical Communication Networks

Dina Reda Elshahat[1,2] · Nihal F. F. Areed[1] · Bedir Yousif[3]

Received: 31 March 2023 / Accepted: 20 April 2023 / Published online: 11 May 2023
© The Author(s) 2023

Abstract
A broadband plasmonic optical modulator based on a dual back-to-back U-shaped silicon waveguide and double layers of graphene has been investigated. The proposed structure is designed at TE mode over a range of wavelengths extending from 1.1 to 1.9 μm**.** By adjusting the geometry of the U-shaped structure, the modulator's performance has been tuned. Utilizing propagation loss, bandwidth, power consumption, and modulation depth, the proposed modulator's performance has been characterized. According to the results, at a wavelength of 1.55 μm, the loss, modulation depth, and small footprint read 0.0415 dB/μm, 0.6337 dB/μm, and (0.5 μm × 12.17 μm), respectively. Furthermore, the proposed modulator has a modulation bandwidth of about 151.7 GHz and a power consumption of 21.068 fJ/bit.

Keywords Graphene · Surface plasmon polaritons · Modulation depth · Modulator

Introduction

One of the essential elements in photonics systems, an optical modulator is a component that modifies a carrier light's basic properties as it travels through an optical waveguide or vacuum in response to an outside photonics or electronics signal [1]. Different designs have been proven to satisfy particular criteria in applications like optical communication, terahertz communication, and current lasers. Advanced-function materials are also becoming increasingly used in the construction of devices as a result of current developments in material science and nanotechnology. To minimize the size of the device and consumption of energy, enhance modulation speed, and increase the range of modulation, hybrid devices have been created by combining germanium, graphene, group III–V elements, and plastics with silicon-based modulators. The types of modulators are polarization, phase, and amplitude modulators based on the characteristics that are being modified. The optical phase of a beam of laser light is controlled by an incoming electromagnetic signal using a phase modulator (PM). Electro-optic modulators based on Pockels cells and LC modulators are two common kinds of PM in the field of integrated optics [2]. Due to its categorized structure, amplitude modulation is typically the most popular. Insertion loss, modulation speed, area efficiency, modulation depth, power consumption, and optical bandwidth can all be used to describe performance [3]. Because of the effect of weak high-order electro-optical, silicon modulators, the primary material used in the semiconductor industry, must be produced on a large scale to achieve sufficient modulation depth. However, germanium- and other compound-based modulators have difficulty integrating with existing complementary metal–oxide–semiconductor (CMOS) technologies. Narrow modulation bandwidth restricts the fabrication of modulators with resonators. The requirements of size, speed, and technique can all be met by graphene, in comparison. Additionally, integrating graphene into current modulators may help them work better. In 2004, mechanical abrasion was used to separate graphene, only a sheet of hexagonally filled atoms of carbon, from graphite. In such extremely restricted crystals that are in two dimensions, the in-plane atoms of carbon are joined by powerful bonds, whereas the layers have weak

✉ Dina Reda Elshahat
Engdina82@yahoo.com

[1] Department of Electronics and Communications Engineering, Faculty of Engineering, Mansoura University, Mansoura 35516, Egypt

[2] Department of Electronics and Communications Engineering, Higher Institute of Engineering and Technology, 41525 New Damietta, Egypt

[3] Department of Electrical Engineering, Faculty of Engineering, Kafrelsheikh University, 35514 Kafrelsheikh, Egypt

van de Waals interactions. Graphene has excellent optical, thermal, mechanical, and electrical characteristics because of its distinctive structure of crystals. The next generation of photonics and electronics is predicted to use graphene as the replacement for silicon. Polarization filters [4], ultrafast lasers, plasmonic structures [5], and photodetectors [6, 7] are just a few examples of photonics devices built on graphene that have been proven.

Graphene offers the following special advantages for use in optical modulators: (1) fast modulation. Graphene has been considered as being one of the foundations of future fast photonics/electronics devices using a carrier velocity of up to 200,000 cm^2/ (V s) at the temperature of a room [1]. Graphene can function at frequencies of more than a hundred GHz thanks to ultrafast (picoseconds) processes like photocarrier production and relaxation. Thus, through gating voltage doping, the Fermi level, which has a direct relation to the graphene's optical absorption, can be quickly modified. (2) Broad optical bandwidth: the constant graphene's optical absorption is $\pi\alpha = 2.293\%$ of wavelengths extending from visible to infrared due to its special electronic structure, where $\alpha = e^2/hc$ refers to the constant of fine-structure [1]. The optical fiber transmission range, which is usually between 1.3 and 1.6 μm, is covered by this bandwidth. (3) High optical absorption: Taking into account a single atom's thickness, the optical absorption of 2.3%, which is about fifty times greater compared to the absorption of GaAs at the identical thickness, is considered to be extremely high. The length of the graphene's light interaction can be increased even more by combining graphene with a waveguide. The footprint, which is the size of the device, is reduced by the higher absorption (4) CMOS-compatible: Large-scale graphene integration using CMOS-compatible techniques has become possible in the last 10 years [1].

Modulators based on graphene have previously been achieved by mixing them with high-index dielectric waveguides. However, in this modulator, the interface between graphene and light has naturally weakened the reason that optical modes are constrained in the region of the dielectric with high-index and far away from the graphene/dielectric waveguide boundary [8].

Surface plasmon polaritons (SPPs) on graphene can be utilized to create outstanding optical modulators for the more constricted spatial containment and intense localized field needed to improve the interaction between light and graphene [9]. For electro-optical modulation, graphene-based hybrid plasmonic modulators have been studied [10]. The modulator's performance can be enhanced by hybrid SPPs, which integrate the extremely small size of the SPP waveguide's mode and the graphene's super-fast speed of modulation. Huang demonstrated a modulator based on hybrid plasmonic graphene [11]. A gap created by the horizontal hybrid plasmonic waveguide was covered with two sheets of one-layer graphene. The gap's effect has increased the modulation bandwidth to 0.4 THz with 8.5 m of modulation length. Theoretically, Peng suggested a modulator based on graphene-on-gap [12]. On the gap of air, a portion of graphene's double layer is hung. Four sheets of one-layer graphene may be modulated over a bandwidth of 0.48 THz with only 3.6 m of modulation length thanks to graphene's linear optical absorption. The device's modulation effectiveness is significantly increased in these modulators by the hybrid plasmonic effect, but fabrication challenges are also present.

This research examines a dual back-to-back U-shaped silicon waveguide-based broadband optical plasmonic modulator using double layers of graphene. The proposed modulator is designed at TE mode for wavelengths varying from 1.1 to 1.9 μm. By modifying the dimensions of the U-shaped, the modulator's performance has been fine-tuned. The performance of the proposed modulator has been characterized using propagation loss, bandwidth, power consumption, and modulation depth. The obtained results show that the loss, modulation depth, and small footprint read 0.0415 dB/μm, 0.6337 dB/μm, and (0.5 μm × 12.17 μm), at a wavelength of 1.55 μm, respectively. Additionally, the proposed modulator offers modulation bandwidth and power consumption of about 151.7 GHz and 21.068 fJ/bit, respectively. Given that graphene has a single-atom-thick, two-dimensional construction, it was considered an anisotropic material [13]. As a result of graphene's constant out-of-plane conductivity ($\sigma_{||}$), the TE mode's properties are considerably affected by slight changes in the graphene's Fermi level, but the mode of TM is not.

Proposed Structure and Physical Explanation

Figure 1a illustrates the cross-sectional view of the suggested modulator. It is seen in Fig. 1a that the suggested design is constructed over a silicon dioxide substrate (0.4 μm × 2 μm) coated with Ag (thick of 0.05 μm and $\varepsilon_r = -129 + 3.3i$ at $\lambda = 1.55$ μm). The waveguide comprises hybrid layers made of a layer of Si ($n = 3.47$) and two layers of graphene and silicon dioxide ($n = 1.445$). A simple capacitor model is created by sandwiching a dielectric spacer called SiO_2 ($d = 7$ nm) between two layers of graphene in the center of the Si waveguide. Au electrodes are attached to two graphene layers to prevent the impact of the gold electrodes on the Si waveguide; the space between the Si waveguide and the gold electrodes was filled with SiO_2. The proposed design has been chosen in its form because the expected power consumption is low. Figure 1b illustrates the magnitude of TE's electric field; the light is typically contained in the medium of a high index in a traditional dielectric waveguide.

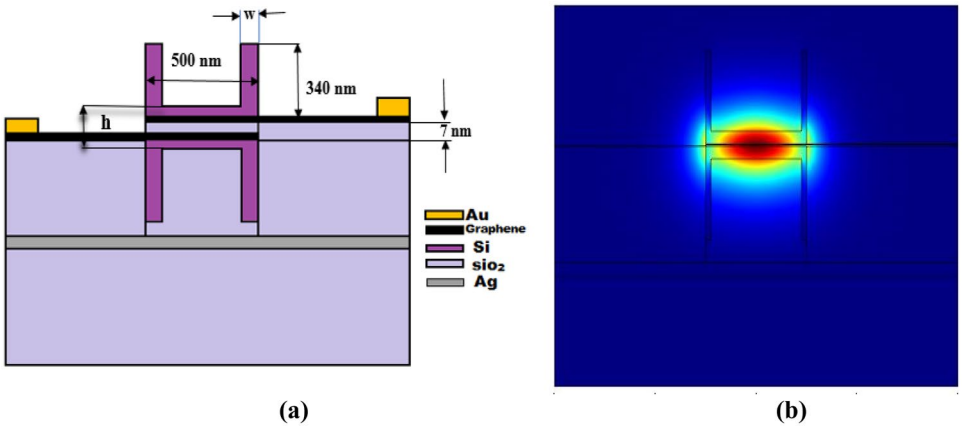

Fig. 1 **a** Graphene-based plasmonic waveguide cross-section. **b** The distribution of electrical field at wavelength 1.55 μm

The suggested modulator's performance is evaluated utilizing optical loss per length (α), propagation loss (PL), and modulation depth (MD). α, PL, and MD are defined here as follows:[14, 15]

$$\alpha = \frac{40\pi(log_{10}\mathrm{e}) * Img\left(n_{eff}\right)}{\lambda} \tag{1}$$

$$PL = \alpha(ON) \tag{2}$$

$$MD = \alpha(OFF) - \alpha(ON) \tag{3}$$

where λ is the incident light wavelength, $\mathrm{Img}(n_{\mathrm{eff}})$ is the effective refractive index's imaginary component, propagation loss is referring to an optical loss per length ("ON" state), and the modulation depth is described as the difference between optical loss per length in the ("OFF") and ("ON") states [16].

The anisotropic electromagnetic characteristics of graphene result from its one-atom-thick, two-dimensional construction. The analytic expression can be used to compute the in-plane conductivity $\sigma_{||}$, and $\sigma\perp$ is the out-of-plane which is similar to that of graphite [17].

$$\sigma_{||} = \sigma_{\mathrm{inter}} + \sigma_{\mathrm{intra}} \tag{4}$$

$$\sigma_{\mathrm{intra}} = \frac{i8\sigma_0}{\pi}\frac{E_{th}}{E_{ph} + iE_S}\ln[2\cosh(\frac{E_f}{2E_{th}})] \tag{5}$$

$$\sigma_{\mathrm{inter}} = \sigma_0[\frac{1}{2} + \frac{1}{\pi}\tan^{-1}\left(\frac{E_{ph} - 2E_f}{2E_{th}}\right) - \frac{i}{2\pi}\ln\frac{(E_{ph} + 2E_{th})^2}{(E_{ph} - 2E_f)^2 + (2E_{th})^2}] \tag{6}$$

where $\sigma_0 = e^2/4\hbar = 60.85(\mu S)$ is the undoped graphene conductivity and $\hbar$ is the constant of reduced Planck, $E_{\mathrm{th}} = k_b T$ (k_b is Boltzmann constant and $T = 300$ K), $E_S = \hbar/\tau$ is the scattering energy, $E_{ph} = \hbar\, c/\lambda$ is the energy of photon, and $\tau = 100$ fs [18]. By using an external voltage, the surface conductivity σg and Fermi level E_f are tuned. The graphene functions like metal and absorbs a lot of light when a low or no voltage is supplied, which is equivalent to the "OFF" state. In contrast, graphene exhibits dielectric behavior when a specific voltage is applied, which is equivalent to the "ON" state. [16]. Equation (5) explains how the applied voltage and the Fermi level are related:

$$E_f = \hbar v_f\sqrt{\pi a_0|V_g - V_0|} \tag{7}$$

where $E_f = \hbar v_f\sqrt{\pi a_0|V_g - V_0|}$ is the graphene's Fermi velocity [19] and $\left|\mathrm{V_g} - \mathrm{V_0}\right|$ is the applied voltage and $a_0 = \varepsilon_r\varepsilon_0/de$ results from the model of a simple capacitor (εr is SiO_2 permittivity, e is the electron's charge, and d is the distance between the simple capacitive planes) [18].

Results and Discussion

Figure 2a shows that when the electrical potential ranges from 0.2872 to 2.5851 V, E_f can be changed from 0.2 to 0.6 eV. The graphene's in-plane permittivity $\varepsilon_{\parallel}$ (E_f) can be computed using

$$\varepsilon_{\parallel}\left(E_f\right) = 2.5 + \frac{i\sigma_{\parallel}}{\omega\varepsilon_0 d_0} \tag{8}$$

The default value of $\varepsilon_{\perp}$ is 2.5 [17], and $d_{\mathrm{o}} = 1$ nm is monolayer graphene thickness [20]. As shown in Fig. 2b, with the Fermi level (E_f) at 1.55 μm, the graphene permittivity has been computed. Both graphene sheets absorb light at $E_f = 0$ eV, which is near the Dirac point. Two graphene layers

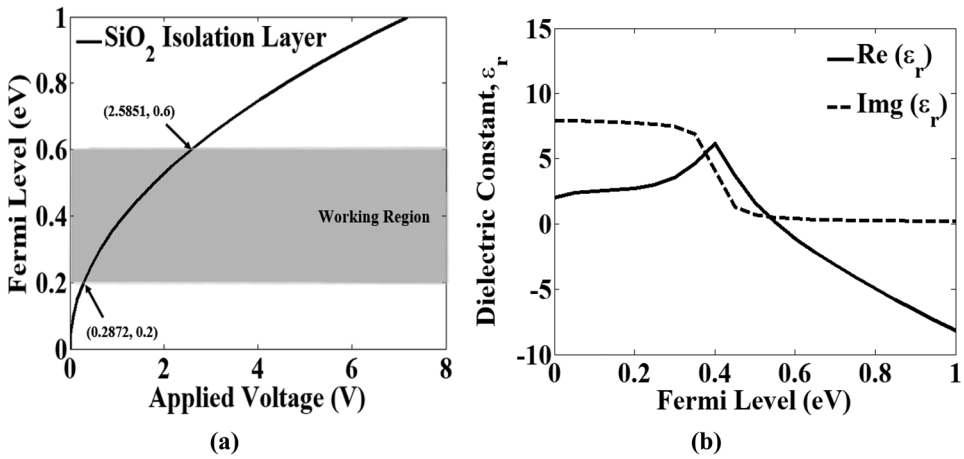

Fig. 2 **a** Variation of the graphene's Fermi level (E_f) with the applied voltage (V), **b** graphene's permittivity for E_f varying from 0 to 1 eV at $\lambda = 1.55$ μm

come together to form a plate capacitor when a voltage is put between them [20]. Both layers of graphene absorb light when they undergo interband transitions at low levels of doping ($E_f < \hbar\nu/2 \approx 0.4$ eV). Both layers turn transparent once the graphene is highly doped ($E_f > \hbar\nu/2 \approx 0.4$ eV), preventing interband transitions. We may therefore create an electro-absorption modulator by using the swing around $E_f = 0.4$ eV.

Table 1 illustrates the initial geometric dimensions of the proposed modulator, and these initial dimensions have been selected to match the operating wavelength range.

According to Fig. 3, the optical loss per length (α) decreases when $E_f = 0.4$ eV, relating to the value of Img(n_{eff}). We put the "OFF" state of the suggested modulator when E_f is below 0.2 eV (the potential difference is less than 0.2872 V) because the optical loss ($\alpha = 0.6335$ dB/μm) is maximum and the design output is reduced. The "ON" state of the proposed modulator is set when E_f is higher than 0.6 eV (the potential difference is less than 2.5851 V) because the optical loss is the lowest possible ($\alpha = 0.0351$ dB/μm) and the design output is maximized. Then, the PL and MD of the suggested modulator are 0.0351 dB/μm and 0.5984 dB/μm, respectively.

We analyze the TE mode's performance of this hybrid waveguide with the changing of dimensions (w and h). Now, we put $w = 50$ nm and h varying from 100 to 660 nm. Figure 4 illustrates the effective mode index (n_{eff}) for h changing from 100 to 660 nm. The TE mode's Re(n_{eff}) increases as h increases, as illustrated in Fig. 4a. Figure 4a shows that with the increase in h, the Img(n_{eff}) of the TE mode is reduced.

Table 1 Initial geometric dimensions of the proposed modulator

Parameters	Values (nm)
h	400
w	50

The relationship between the optical modulator's performance and h is shown in Fig. 5. The modulation depth of TE mode decreased as h increased, as shown in Fig. 5a. According to Fig. 5b, with the increase in h from 100 to 660 nm, the propagation loss decreased. However, increasing h causes MD and PL to decrease. As a result, h of about 100 nm is chosen to achieve the highest MD of about 0.5954 dB/μm. The propagation loss reads of about 0.03844 dB/μm, as shown in Fig. 5a, which is acceptable in comparison with previous studies.

After that, we put h at 100 nm, and concentration on the optimization of the thickness of w. Figure 6 illustrates the effective mode index (n_{eff}) of "ON" and "OFF" states with

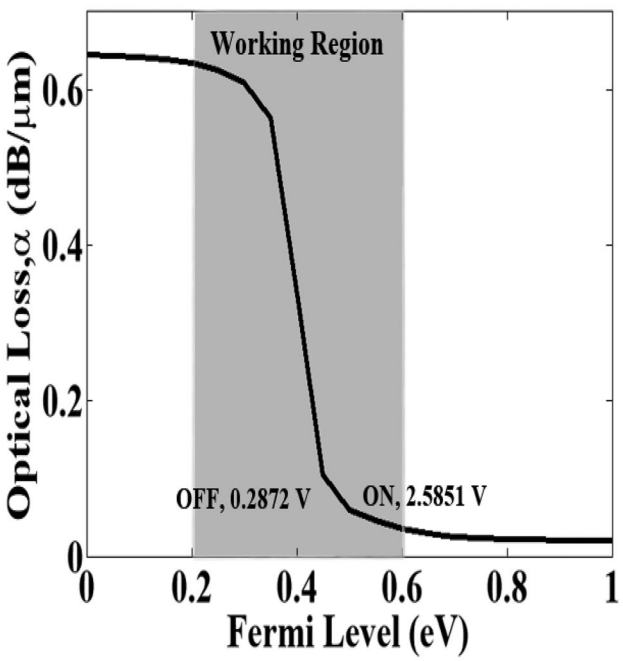

Fig. 3 Relationship between the optical loss per length of TE mode and the Fermi level for the initial geometric dimensions

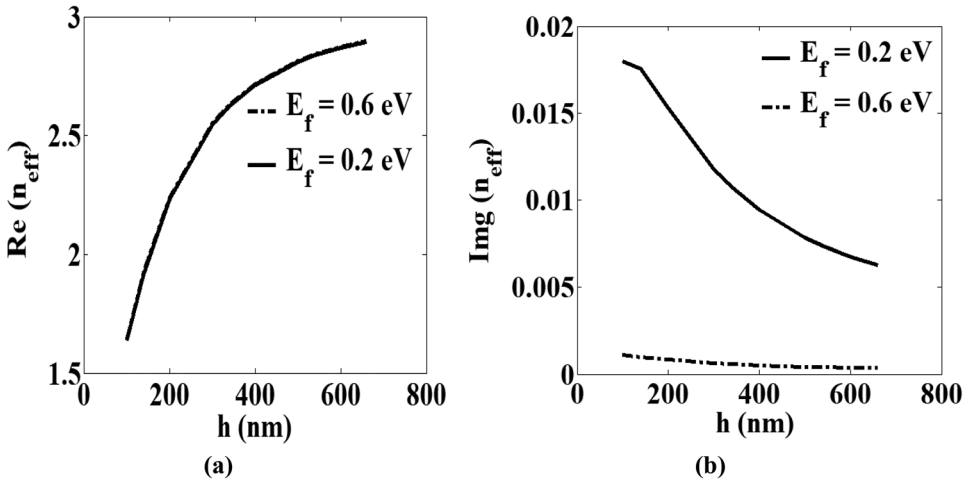

Fig. 4 The relationship between **a** real and **b** imaginary component of TE mode and *h*

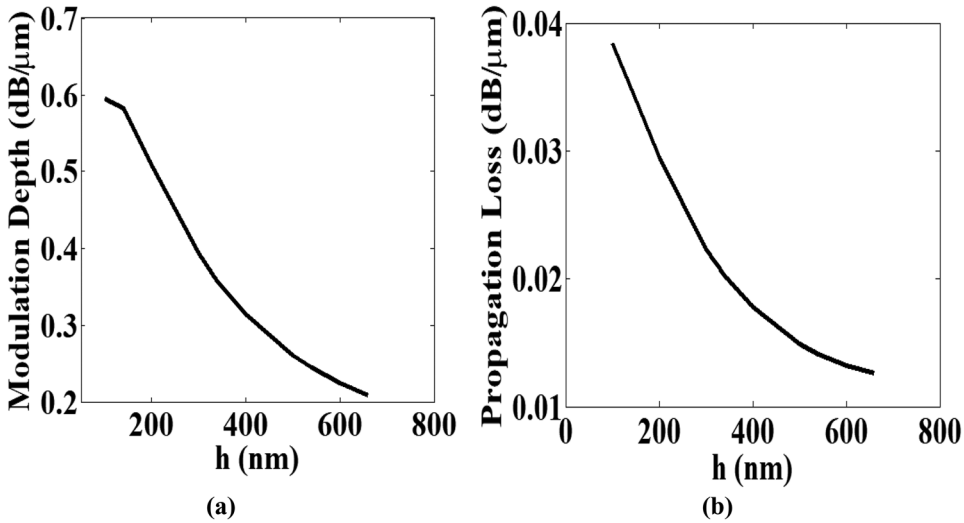

Fig. 5 **a** Modulation depth. **b** The propagation loss as a function of h

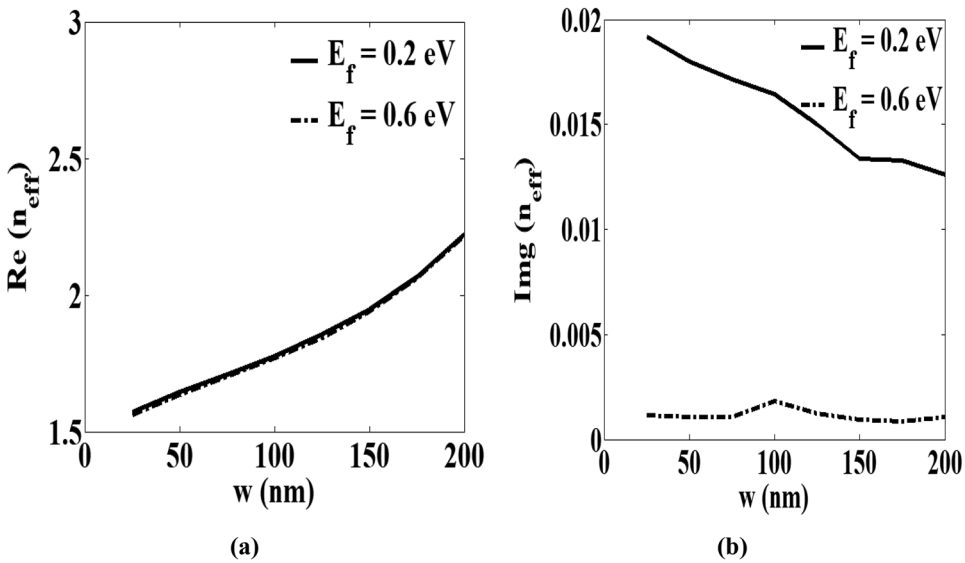

Fig. 6 **a** Real and **b** imaginary component of TE mode with respect to *w*

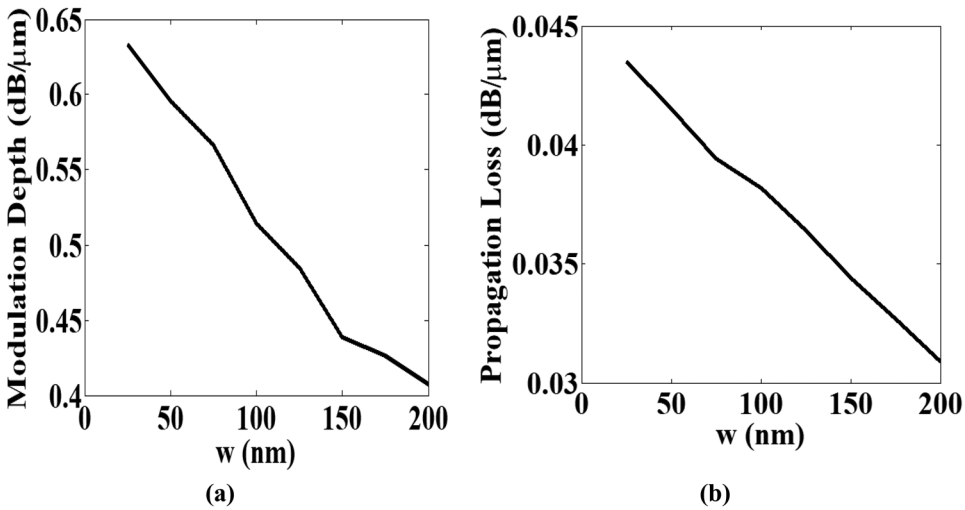

Fig. 7 **a** Modulation depth. **b** The propagation loss with respect to *w*.

respect to *w*. The TE mode's Re(n_{eff}) rises as *w* increases, as illustrated in Fig. 6a. The TE mode's Img(n_{eff}) decreases with the change of *w* from 25 to 200 nm as shown in Fig. 6b.

Figure 7 shows the PL and MD as a function of w. As shown in Fig. 7a, as the w rises, MD declines and has a minimum value of 0.4073 dB/μm at $w = 200$ nm. Figure 7b shows the relation between the propagation loss and *w*, which decreases with the increase of *w*. We choose $w = 25$ nm due to its relatively higher MD of about 0.6337 dB/μm and acceptable propagation loss of about 0.0415 dB/μm.

Table 2 illustrates the tuned geometric dimensions of the suggested modulator. In the following subsection, the characterization parameter: the effective mode index (n_{eff}), propagation loss, optical bandwidth, frequency response, and energy consumption are calculated for the suggested modulator with tuned geometry.

Effective Mode Index (n_{eff})

It investigated how modulation performance and Fermi level relate to one another. The relation between the effective mode index (n_{eff}) and the Fermi level is shown in Fig. 8. By varying the graphene's Fermi level, the Re(n_{eff}) and Img(n_{eff}) can be changed. As shown in Fig. 8a when E_f changes from 0 to 1 eV, Re(n_{eff}) first increases to its greatest value at $E_f = 0.4$ eV ($\hbar\nu/2$) and subsequently decreases. Figure 8b shows when $E_f > 0.4$ eV, Img(n_{eff}) exhibits a sharp decline around $E_f = 0.4$ eV, according to the graphene Pauli blocking mechanism.

Table 2 Tuned geometric dimensions of the proposed modulator

Parameters	Values (nm)
h	100
w	25

Propagation Loss

Figure 9 illustrates the optical loss per length (α) for E_f varying from 0 to 1 eV. According to Fig. 9, the maximum optical loss is (α (OFF) = 0.6752 dB/μm), and the minimum optical loss is (α (ON) = 0.0415 dB/μm). Then, the MD and PL of the proposed design read 0.6337 dB/μm and 0.0415 dB/μm, respectively.

Optical Bandwidth

Figure 10 illustrates graphene's dielectric constant with respect to the wavelength of incident light. Figure 10a shows the relationship between Re (ε_r) and Img (ε_r) of graphene and the wavelength of incoming light at $E_f = 0.2$ eV. The relationship between Re (ε_r) and Img (ε_r) of graphene and the wavelength of incoming light at $E_f = 0.6$ is shown in Fig. 10b.

Figure 11 illustrates the effective mode index (n_{eff}) with respect to wavelength. As shown in Fig. 11a, the Re(n_{eff}) declines as wavelength increases. The greatest Re(n_{eff}) value for the TE mode at $\lambda = 1.1$ μm and $E_f = 0.6$ eV is 2.0694. The value of Re(n_{eff}) of the TE mode is 2.063 at $\lambda = 1.1$ μm and $E_f = 0.2$ eV. The value of Re(n_{eff}) of the TE mode is 1.2138 at $\lambda = 1.9$ μm and $E_{f=}$ 0.6 eV. The Re(n_{eff}) value of the TE mode is 1.2297 at $\lambda = 1.9$ μm and $E_{f=}$ 0.2 eV.

As depicted in Fig. 11b, it has been found that when the wavelength ranges between 1.1 and 1.9 μm at $E_f = 0.6$ eV, the Img(n_{eff}) of the TE mode changes from 0.0036176 to 0.001344. The mode's Img(n_{eff}), which ranges between 0.01748 to 0.018875 at $E_f = 0.2$ eV, is mostly caused by the improvement of the light interaction of graphene as a result of rising dielectric constant with increasing wavelength.

According to Fig. 12a, the modulation depth changes with wavelength. As is obvious, the MD of the suggested modulator read 0.6877 dB/μm at $\lambda = 1.1$ μm and reaches its maximum at $\lambda = 1.2$ μm then dropped to 0.5036 dB/μm at

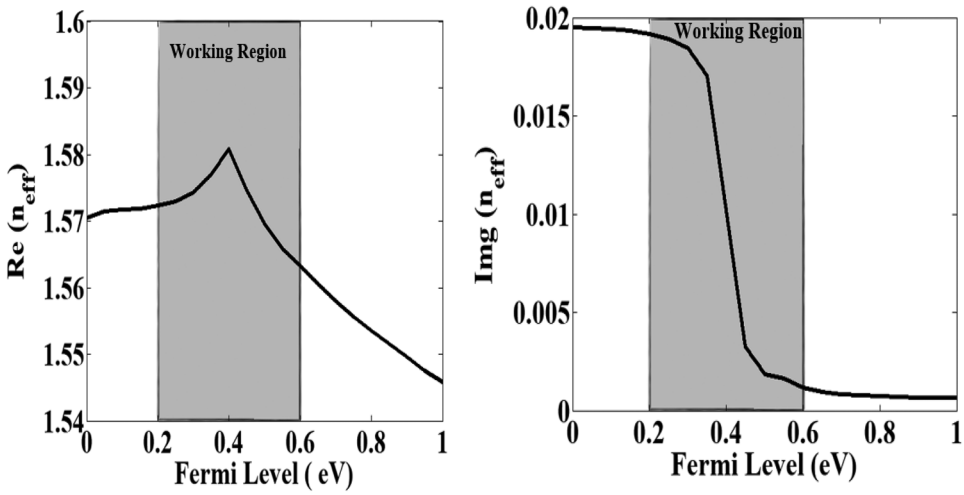

Fig. 8 The relationship between **a** real and **b** imaginary component of TE mode and the Fermi level

$\lambda = 1.9$ μm, which is still a large number. As a result, the suggested modulator operates as a broadband modulator and has an acceptable MD of 0.7371 dB/μm to 0.5036 dB/μm in the range of wavelength from 1.2 to 1.9 μm. Additionally, the modulation depth of our suggested modulator at 1.55 μm wavelength is 0.6337 dB/μm.

Figure 12b shows the change of optical loss per length with wavelength extending from 1.1 to 1.9 μm at two values of the Fermi level. At a wavelength of 1.1 μm, the loss in Fermi level of 0.6 eV has a value of 0.1795 dB/μm, and it has reached 0.0415 dB/μm at the telecommunication wavelength of 1.55 μm, and it has also attained 0.0386 dB/μm at the wavelength of 1.9 μm. In the wavelength extending from 1.1 to 1.9 μm, it is seen that there is little change in the loss. As a result, the suggested modulator has broadband modulation capabilities.

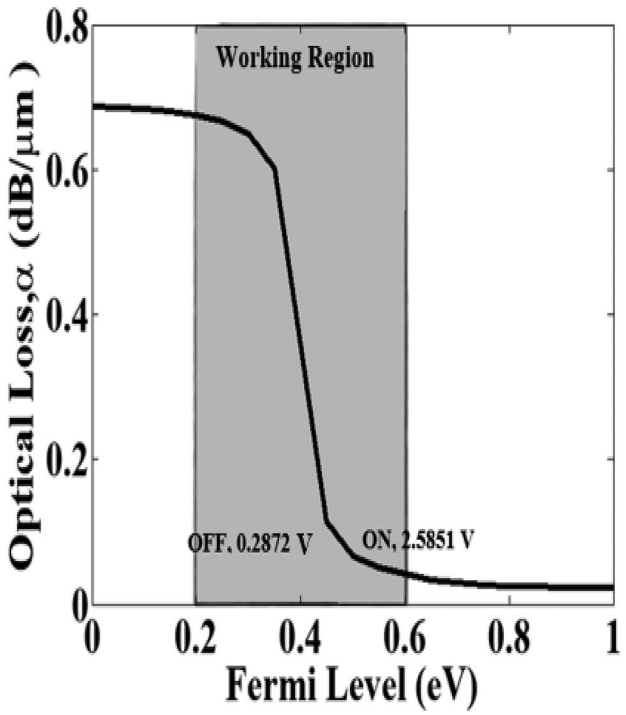

Fig. 9 Optical loss per length versus Fermi level, E_f for the final geometric dimensions

Frequency Response and Power Consumption

For an electro-optical modulator, the modulation bandwidth and consumption of energy are also two significant metrics of performance. Figure 13 illustrates how we created the modulator model similar to the circuit model to compute the frequency response and power dissipation. To calculate the frequency response and power dissipation, we made the modulator model equivalent to the circuit model, which is shown in Fig. 13. The modulation bandwidth can be estimated by $F_{3dB} = \frac{1}{2\pi RC}$ [20, 21] where the capacitance $C = \frac{\epsilon_r \epsilon_0}{Sd}$ can be determined using graphene—SiO_2—graphene geometry of the model for parallel capacitance, ϵ_r is the relative insulating dielectric spacer's permittivity, d denotes the isolating dielectric gap thickness between the layers of graphene, and S is the graphene layer area. The material and thickness of the insulating dielectric spacer significantly affect the 3-dB modulation bandwidth as well as the consumption due to the presence of bilayer graphene. As a result, it is essential to alter the insulating dielectric spacer's material and thickness to maximize the modulator's performance [31]. [31] used two types of materials hBN ($\varepsilon_r = 3.92$) and Al_2O_3 ($\varepsilon_r = 7$) and studied the influence of the thickness on the modulator performance. From the results, it was found that when using hBN as an insulating material, it achieves high bandwidth and low energy consumption when hBN was used as an insulator material with a thickness of (7 nm). In this study, SiO_2

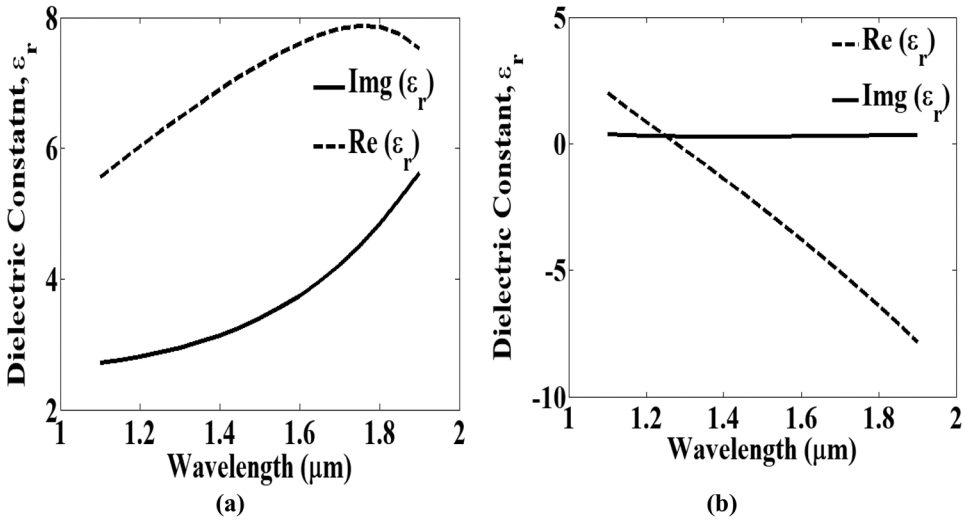

Fig. 10 The dielectric constant for two Fermi level values as a function of wavelength **a** "OFF" and **b** "ON" states

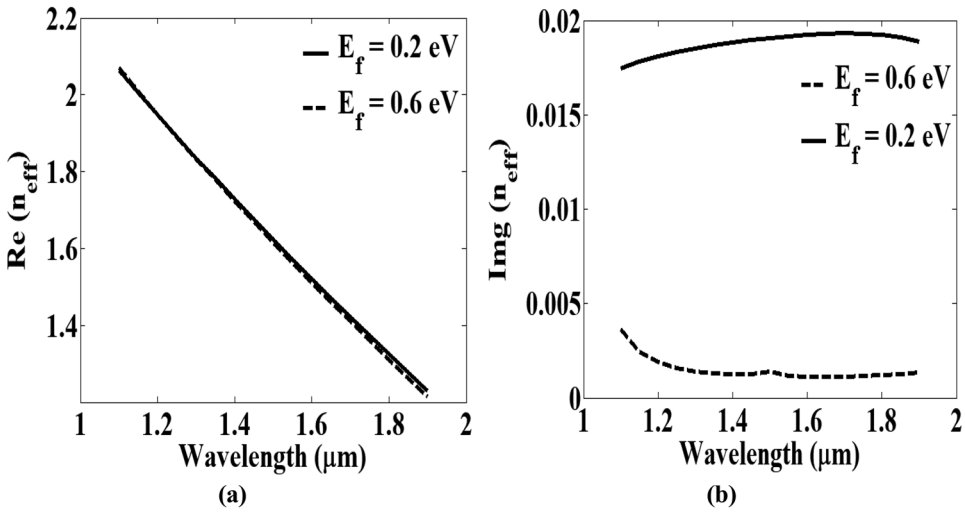

Fig. 11 The relationship between **a** $Re(n_{eff})$, **b** $Img(n_{eff})$, and the wavelength

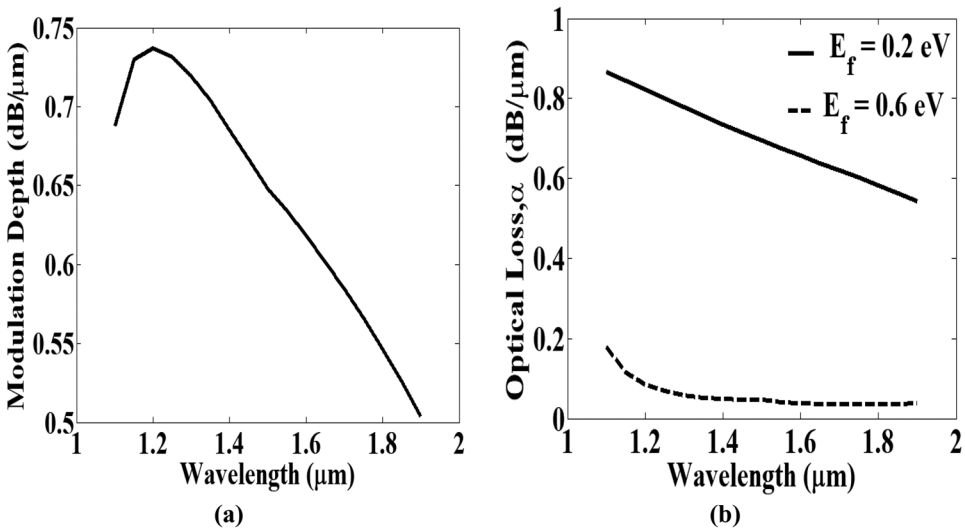

Fig. 12 **a** Modulation depth. **b** Optical loss per length as a function of wavelength

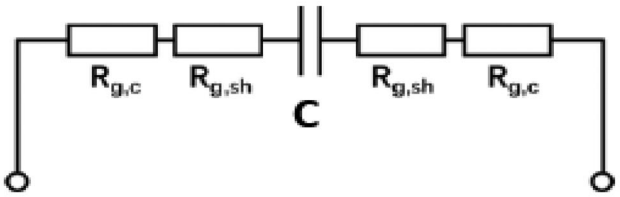

Fig. 13 The equivalent circuit model for bandwidth estimation

was used as an insulator material with a thickness of 7 nm because it gave better results than in paper [31], in addition to reducing the number of materials used in the design.

The resistance R comprises the resistance of graphene sheet R_G and the resistance of graphene-electrode contact R_c, and $R_{c=}$ 400 Ωμm is the main factor [31]. Therefore,

$$F_{3dB} = \frac{1}{2\pi RC} = \frac{1}{2\pi\left(R_C + R_G\right)C} \approx \frac{1}{2\pi R_C C} \tag{9}$$

The power consumption is calculated by $E_{bit} = \frac{1}{4}C\Delta V^2$, and ΔV is dependent on the applied voltage for the modulator's "ON" and "OFF" states [15]. The hybrid plasmonic waveguide length is selected to be 12.17 μm according to [20]. Based on this selection, the modulation bandwidth and the power consumption read 151.7 GHz and 21.068 fJ/bit, respectively.

Comparison with Previous Modulator Designs

Table 3 compares the performance of the suggested modulator with other previously reported modulators. The comprised items are modulation depth, power consumption, loss, and bandwidth. According to Table 3, the proposed modulator has a modulation bandwidth that is higher than previous research at about 151.7 GHz. The power consumption and the loss are lower than the other modulators as well ([16, 20], and [31]). Additionally, the suggested modulator shows the highest MD of about 0.6337 dB/μm which represents approximately six hundred in comparison with [22] and [24] and approximately two hundred in comparison with [20, 25], and [27].

Table 3 Comparing the modulator's performance with published works

Ref	MD (dB/μm)	F_{3dB} (GHz)	Loss (dB/μm)	Ebit (fJ/bit)
[22]	0.1	1	-	-
[23]	0.16	1	0.1	1000
[24]	0.1	35	-	1400
[25]	0.28	30	0.05	100
[26]	0.41	46.4	0.42	630
[27]	0.2975	30.2	-	2980
[28]	0.06	13.4	-	-
[29]	0.08	80	-	-
[30]	0.52	95	0.03401	138.8
[20]	0.246	80	6.77	108.8
[31]	-	190.5	0.58	14
[32]	0.2	21.2	0.2	52.7
[16]	0.502	127	0.07306	72
This work	0.6337	151.7	0.0415	21.068

Conclusion

A dual back-to-back U-shaped silicon waveguide and double layers of graphene were used to create a wideband optical plasmonic modulator, which has been investigated. The proposed modulator's performance has been characterized using propagation loss (PL), bandwidth, power consumption, effective mode index (n_{eff}), and modulation depth (MD). Studies have been done on how the Fermi level and wavelength affect these elements. An optical absorption TE modulator with great performance has been proposed with a compact size (12.17 μm × 0.5 μm) and low consumption of energy of about 21.068 fJ/bit. Moreover, high modulation bandwidth of about 151.7 GHz with a low propagation loss of about 0.0415 dB/μm. Our design shows excellent promise for creating new integrated optical devices.

Author Contribution All authors contributed to the study conception and design. Material preparation, data collection analysis, prototype design model, simulation, and results interpretation were performed by Dina Reda Elshahat, Nihal F.F. Areed, and Bedir Yousif. The first draft of the manuscript was written by Dina Reda Elshahat, Bedir Yousif, and Nihal F.F, and all authors commented on previous versions of the manuscript. All authors read and approved the final manuscript.

Funding Open access funding provided by The Science, Technology & Innovation Funding Authority (STDF) in cooperation with The Egyptian Knowledge Bank (EKB).

Data Availability All data is available and will be provided upon request by the corresponding author.

Declarations

Ethics Approval In this study, no ethical approval is required.

Consent to Participate Not applicable.

Consent for Publication Not applicable.

Competing Interests The authors declare no competing interests.

Open Access This article is licensed under a Creative Commons Attribution 4.0 International License, which permits use, sharing, adaptation, distribution and reproduction in any medium or format, as long as you give appropriate credit to the original author(s) and the source, provide a link to the Creative Commons licence, and indicate if changes

were made. The images or other third party material in this article are included in the article's Creative Commons licence, unless indicated otherwise in a credit line to the material. If material is not included in the article's Creative Commons licence and your intended use is not permitted by statutory regulation or exceeds the permitted use, you will need to obtain permission directly from the copyright holder. To view a copy of this licence, visit http://creativecommons.org/licenses/by/4.0/.

References

1. Luo S, Wang Y, Tong X, Wang Z (2015) Graphene-based optical modulators. Nanoscale Research 10:199–211
2. Areed NF, Obayya SS (2014) Multiple image encryption system based on nematic liquid photonic crystal layers. J Light Technol 32(7):1344–1350
3. Reed GT, Mashanovich G, Gardes FY, Thomson DJ (2011) Silicon optical modulators Nat Photon 4:518–526
4. Almewafy BH, Areed NF, Hameed MF, Obayya SS (2019) Modified D-shaped SPR PCF polarization filter at telecommunication wavelengths. Opt Quant Electron 51:193
5. Hussein M, Areed NFF, Hameed MFO, Obayya SSA (2014) Hybrid core semiconductor nanowires for solar cell applications Numerical Simulation of Optoelectronic Devices. Palma de Mallorca, Spain, pp 89–90
6. Novoselov KS, Geim AK, Morozov SV, Jiang D, Katsnelson MI, Grigorieva IV et al (2005) Two-dimensional gas of massless Dirac fermions in graphene. Nature 438:197–200
7. El-Rabiaey MA, Areed NF, Obayya SS (2016) Novel plasmonic data storage based on nematic liquid crystal layers. J Light Technol 43:3726–3732
8. Zhu Y, Deng C, Huang L, Hu G, Yun B, Zhang R, Cui Y (2020) Hybrid plasmonic graphene modulator with buried silicon waveguide. Opt Commun 456:124559
9. Huang L, Hu G, Deng C, Zhu Y, Yun B, Zhang R, Cui Y (2018) Realization of mid-infrared broadband absorption in monolayer graphene based on strong coupling between graphene nanoribbons and metal tapered grooves. Opt Express 26(22):29192
10. Zheng P, Yang H, Fan M, Hu G, Zhang R, Yun B, Cui Y (2018) A hybrid plasmonic modulator based on graphene on channel plasmonic polariton waveguide. Plasmonics 11468
11. Huang BH, Lu WB, Li XB, Wang J, Liu ZG (2016) Waveguide-coupled hybrid plasmonic modulator based on graphene. Appl Opt 55(21):5598
12. Peng X, Hao R, Ye Z, Qin P, Chen W, Chen H, Jin X, Yang D, Li E (2017) Highly efficient graphene-on-gap modulator by employing the hybrid plasmonic effect. Opt Lett 42(9):1736
13. Shin J-S, Kim JT (2015) Broadband silicon optical modulator using a graphene-integrated hybrid plasmonic waveguide. Nanotechnology 26:365201
14. Karimkhani H, Vahed H (2022) A broadband optical modulator based on rib-type silicon waveguide including graphene and h-BN layers. Optik - International Journal for Light and Electron Optics 254:168633
15. Karimkhani H, Vahed H (2020) Hybrid broadband optical modulator based on multi-layer graphene structure and silver nanoribbons. Opt Quant Electron 52:229
16. Liu S, Wang M, Liu T, Xu Y, Yue J, Yi Y, Sun X, Zhang D (2022) Polarization-insensitive graphene modulator based on hybrid plasmonic Waveguide Photonics 9:609
17. Kwon MS (2014) Discussion of the epsilon-near-zero effect of graphene in a horizontal slot waveguide. IEEE Photon J 6
18. Wang F, Zhang Y, Tian C, Girit C, Zettl A, Crommie M, Shen YR (2008) Gate variable optical transitions in graphene. Science 320:206–209
19. Hwang C, Siegel DA, Mo SK, Regan W, Ismach A, Zhang Y, Zettl A, Lanzara A (2012) Fermi velocity engineering in graphene by substrate modification. Sci Rep 2:590–593
20. Lu Y, Cai K, Li Y, Duan Z, Xi Y, Wang Z (2019) A high speed optical modulator based on graphene-on-graphene hybrid nanophotonic waveguide. Optik - Int J Light Electron Opt 179:216–221
21. Mescia L (2015) Innovative materials and systems for energy harvesting applications§
22. Liu M, Yin X, Ulin-Avila E, Geng B, Zentgraf T, Ju L et al (2011) A graphene-based broadband optical modulator. Nature 474:64–67
23. Liu M, Yin X, Zhang X (2012) Double-layer graphene optical modulator. Nano Lett 12:1482–1485
24. Dalir H, Xia Y, Wang Y, Zhang X (2016) Athermal broadband graphene optical modulator with 35 GHz speed. Acs Photon 3(9):1564–1568
25. Kovacevic G, Yamashita S (2016) Design optimizations for a high-speed two-layer graphene optical modulator on silicon". IEICE Electr Expr 13(14):20160499–20160499
26. Kim Y, Kwon M-S (2017) Electroabsorption modulator based on inverted-rib-type silicon waveguide including double graphene layers. J Opt 19(4):045804
27. Hu X, Wang J (2018) Design of graphene-based polarization-insensitive optical modulator Nanophotonics 7:651–658
28. Yang Z, Lu R, Cai S, Wang Y, Liu Y (2019) A CMOS-compatible and polarization-insensitive graphene optical modulator Opt. Commun 450:130–135
29. Yang Z, Lu R, Wang Y, Cai S, Zhang Y, Wang X, Liu Y (2019) A fabrication-friendly graphene-based polarization insensitive optical modulator. Optik 182:1093–1098
30. Shirdel M, Mansouri-Birjandi MA (2019) Broadband graphene modulator based on a plus-shaped plasmonic slot waveguide Appl. Optics 58:8174–8179
31. Vahed H, Ahmadi SS (2020) Hybrid plasmonic optical modulator based on multi-layer graphene. Opt Quantum Electron 52(1):1–11
32. Karimkhani H, Vahed H (2021) An optical modulator with ridge-type silicon waveguide based on graphene and MoS2 layers and improved modulation depth. Opt Quantum Electro 53:211–220

Publisher's Note Springer Nature remains neutral with regard to jurisdictional claims in published maps and institutional affiliations.